

Laue and Kossel Diffraction on Quasicrystals by Means of Synchrotron Radiation

Ch. Schetelich,^a S. Brenner^b and V. Geist^{c*}

^aPhysics Department, University of Warwick, Coventry CV4 7AL, UK, ^bETH Zürich, Lab. für Kristallographie, ETH-Zentrum, CH-8092 Zürich, Switzerland, and ^cUniversität Leipzig, Institut für Mineralogie, Kristallographie und Materialwissenschaft, D-04275 Leipzig, Germany.
E-mail: geist@rz.uni-leipzig.de

(Received 10 July 1997; accepted 25 November 1997)

Laue experiments using synchrotron radiation have been carried out on quasicrystalline samples mainly with decagonal symmetry. Apart from Laue spots, Kossel lines and diffuse scattering have been observed on the X-ray film simultaneously. High spatial resolution was achieved by the positioning of the X-ray film at a distance of about 350 mm from the sample. Conclusions about the real structure and the crystal quality could be drawn using information obtained from the appearance of the Kossel lines, and the shape and the splitting of the Laue spots, respectively. The dimensions of the mosaic blocks and their tilting behaviour for one of the samples under investigation have been determined.

Keywords: quasicrystals; Kossel effect; Laue diffraction; diffuse scattering; mosaic structure.

1. Introduction

If an X-ray film is placed close to a single crystal and the crystal acts as a target for an intense white X-ray beam, two different diffraction patterns can be observed simultaneously on the film. Firstly, the well known Laue spots, and secondly, so-called Kossel lines. In contrast to the Laue spots, Kossel interferences are generated by the characteristic X-ray fluorescence radiation excited by the primary beam (Fig. 1). Borrmann has already proved the occurrence of this effect with copper single crystals and other materials in 1936 (Borrmann, 1936). To generate Kossel lines only, usually an electron beam of energy between 20 and 50 keV is used to excite the characteristic X-ray radiation. The advantages of this method are the short exposure times and very small probe diameters compared with the beam diameter of a conventional X-ray source. Usually, a scanning electron microscope serves as the electron source. Only the advent of synchrotrons and the resulting highly intense X-ray radiation permitted sufficiently short exposure times together with a better angular resolution. The latter was achieved because of the increased distance between the sample and the film (Ullrich *et al.*, 1994; Schetelich *et al.*, 1995). Using a monochromator it was even possible to excite selectively the characteristic radiation of a certain kind of atom, *e.g.* the exclusive excitation of Ga $K\alpha$ radiation in GaAs crystals. The main advantage of this is the reduction of unwanted background radiation.

It should be mentioned here that the profiles of Kossel lines excited by synchrotron radiation have also been

investigated using solid-state detectors instead of X-ray film (Takahashi & Takahashi, 1993; Gog *et al.*, 1995).

A special feature of the Kossel effect is the occurrence of a fine structure of the Kossel lines (*e.g.* 'light-dark'). This is the result of a superposition process of primary and secondary beams (Fig. 1) and is closely related to the conservation of the scattering phase. Therefore, the occurrence of this fine structure is a dynamical phenomenon and a high degree of structural order in the region investigated is required. The entire Kossel pattern itself contains information about lattice parameters, orientation and symmetry. However, the low intensities of the Kossel lines, usually a few percent of the non-diffracted background, sometimes cause problems in the recording process. In synchrotron experiments performed earlier (Schetelich *et al.*, 1995) conventional crystals (CuO₂, CuSO₄, GaAs, GaP) were investigated. On the other hand, the electron-induced Kossel effect has already proved useful for the investigation of decagonal quasicrystals (Schetelich *et al.*, 1994). Therefore, the application of synchrotron radiation to excite Kossel interferences in decagonal quasicrystals† seems straightforward. Except for other spectacular properties, decagonal quasicrystals show strong diffuse scattering. Therefore, the observation of three different kinds of diffraction phenomena (Laue

† The structure of these quasicrystals shows periodical stacking of planes in one direction (tenfold screw axis). Within the planes there is no translational order, but quasiperiodicity or orientational order is exhibited. To index the diffraction patterns of quasicrystals, more than three indices are required; in the case of a decagonal quasicrystal, four for indexation within the quasiperiodical planes and one for the periodical direction, *i.e.* five altogether (*e.g.* Steurer, 1990) are required.

spots, Kossel lines and diffuse scattering) was expected for the characterization of the samples.

2. Experimental

Two different decagonal quasicrystalline samples with the nominal compositions $\text{Al}_{70}\text{Co}_{15}\text{Ni}_{15}$ and $\text{Al}_{62}\text{Co}_{15}\text{Cu}_{20}\text{Si}_3$ were investigated. The samples exhibit a decaprismatic needle-like shape with dimensions ranging from 0.3 mm in diameter and a length of about 1.5 mm for the

$\text{Al}_{70}\text{Co}_{15}\text{Ni}_{15}$ crystal up to 2 mm in diameter and 4 mm in length in the case of the $\text{Al}_{62}\text{Co}_{15}\text{Cu}_{20}\text{Si}_3$ crystal.

All experiments were performed at beamline F1 at HASYLAB, DESY, using white synchrotron radiation. The samples were mounted on a four-circle diffractometer in order to simplify the alignment procedure. In both cases the tenfold axis was orientated parallel to the z direction as indicated in Fig. 1(c). The recordings were taken in back-reflection geometry. High spatial resolution was achieved by placing the film at a distance of 350 mm from the sample. The experimental pattern covers a horizontal angular region of approximately $18\text{--}22^\circ$. The size of the incident beam could be varied between about $50 \times 50 \mu\text{m}^2$ and $250 \times 250 \mu\text{m}^2$ by means of a double-slit aperture. Typical exposure times on Fuji X-ray film IX100 and IX150, respectively, lasted from a few seconds for the largest aperture opening up to about 30 min for the smallest. Initially, we tried to use image plates in order to avoid the time-consuming film processing of the X-ray film.

However, the quality of the images has been not as good as expected. Therefore, X-ray film had to be used instead. Nevertheless, for alignment purposes the image plates proved very useful.

3. Results and discussion

Laue spots and diffuse scattering in the form of a straight horizontal line have been recorded for both samples and all beam sizes. The Laue spots connected by the diffuse line(s)† have a general indexation of $\{hkml0\}$ (Kek & Mayer, 1993). As soon as the beam dimensions became smaller than approximately $70 \times 70 \mu\text{m}^2$, Kossel lines could also be observed (Figs. 2a and 2b). This means we have obtained three different independent sources of information from one recording simultaneously.

Comparing the images taken from the two samples, quite large differences in quality were found. $\text{Al}_{70}\text{Co}_{15}\text{Ni}_{15}$ shows extremely sharp reflections in contrast to $\text{Al}_{62}\text{Co}_{15}\text{Cu}_{20}\text{Si}_3$. Here, a multiple split line of diffuse scattering, broad and rather diffuse Kossel lines and Laue reflections occurred. In Fig. 2(c) a simulation of the Kossel pattern of Fig. 2(b) is given. From this Kossel pattern, lattice parameters and the sample orientation could be determined [$c = 0.3772 \text{ nm}$, $a = 0.4143 \text{ nm}$, the orientation pole corresponds to (24221)].

The $\text{Al}_{70}\text{Co}_{15}\text{Ni}_{15}$ sample has been the subject of a series of detailed investigations and can be considered as a 'true and almost perfect' quasicrystal within the experimental limit (Kalning *et al.*, 1995). The observation of Kossel lines showing the typical fine structure (Fig. 2a) confirms once more the occurrence of dynamical X-ray diffraction in real quasiperiodic structures, and not only in their crystalline

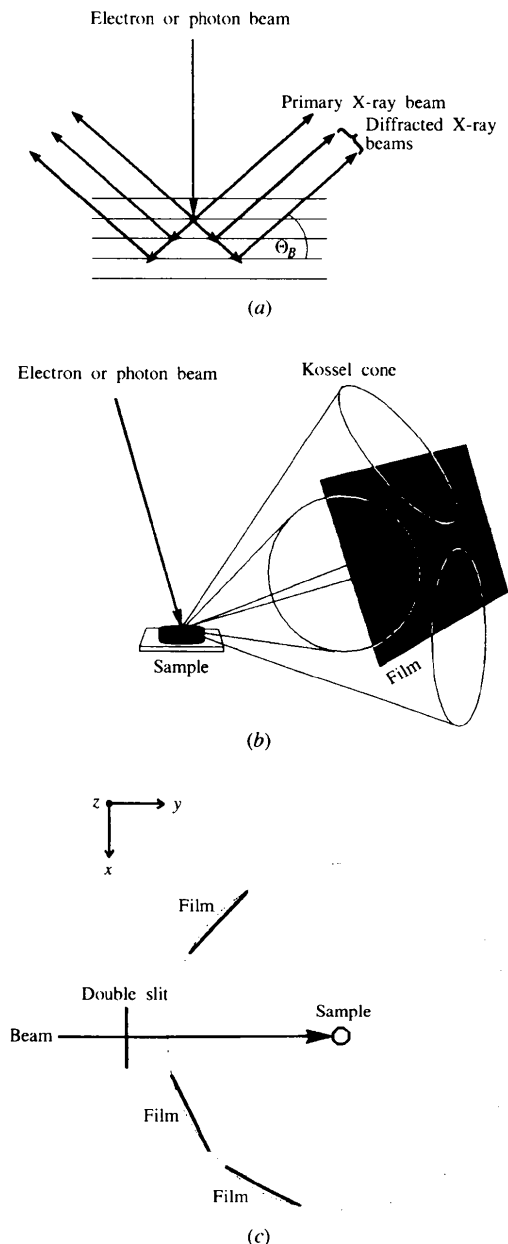


Figure 1

(a) Excitation and diffraction schemes of characteristic X-rays. (b) Kossel lines obtained as the intersection of Kossel cones with X-ray film, in 'flat film' geometry. (c) Experimental set-up. The z axis is normal to the plane of the electron motion in the storage ring.

† It should be mentioned that a distinction between the diffuse scattering within the Bragg layers and that originating from between two Bragg layers cannot be made by the Laue technique.

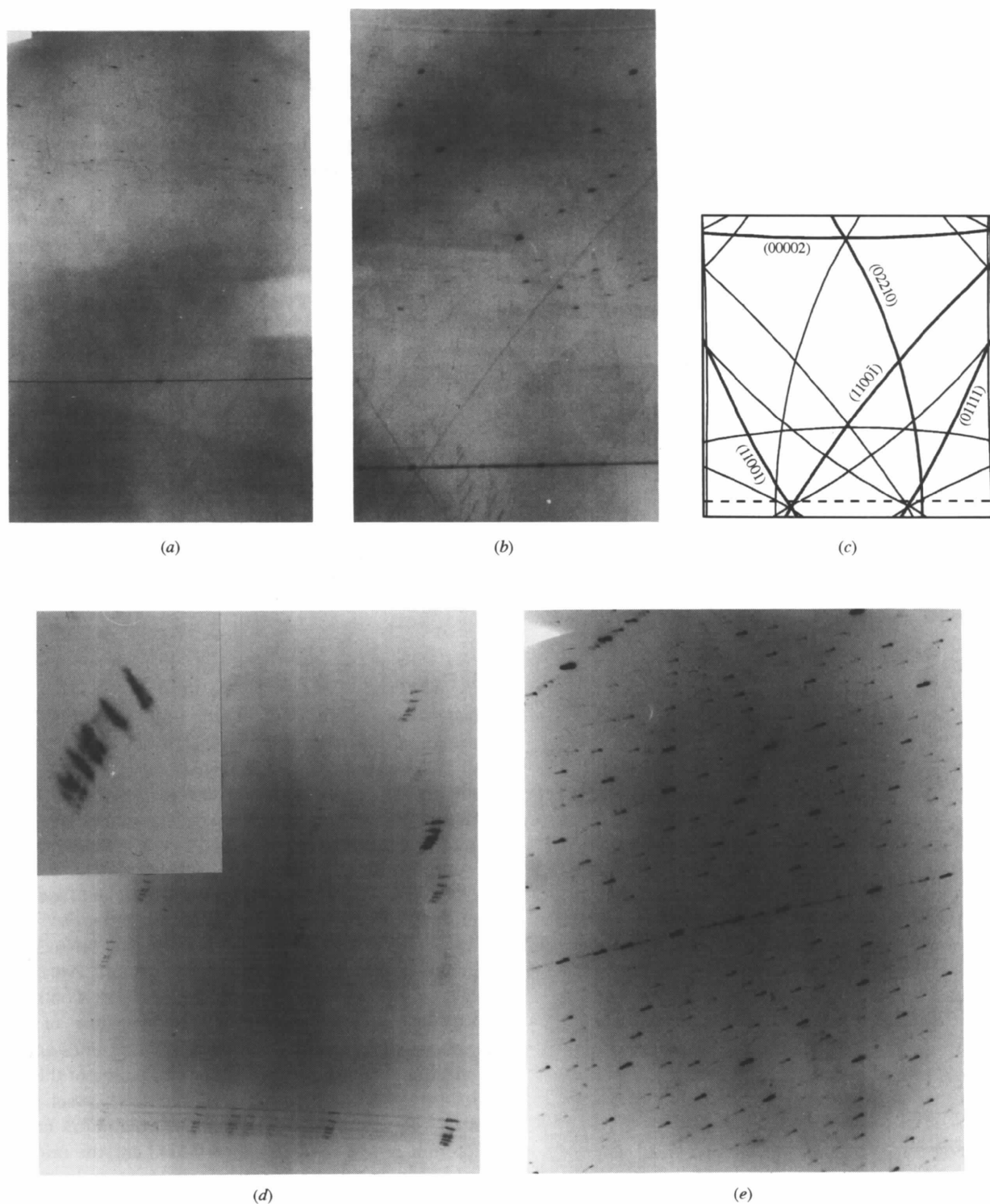


Figure 2

(a) Kossel pattern obtained from the $\text{Al}_{70}\text{Co}_{15}\text{Ni}_{15}$ sample. The beam size was smaller than $70 \times 70 \mu\text{m}^2$. Kossel reflections appear as double lines due to $\text{Co } K\alpha$ and $\text{Ni } K\alpha$ radiation. Additionally, Laue reflections and the diffuse scattering in the form of a distinct horizontal line are visible. (b) As (a) but using an $\text{Al}_{62}\text{Co}_{15}\text{Cu}_{20}\text{Si}_3$ quasicrystal. Note that all 'signals' are broader than in (a). Furthermore, the double lines are not equal in intensity; $\text{Co } K\alpha$ reflections are stronger than Cu reflections. (c) Calculated Kossel pattern according to conditions (b). For clarity, only the $\text{Co } K\alpha$ lines are shown. The lattice parameters determined therefore are $c = 0.4143 \text{ nm}$ and $a = 0.3772 \text{ nm}$. For the orientation of the simulation we obtain the indexation 24221. Not all lines drawn in the simulation are visible on the corresponding Kossel pattern. The position of the diffuse line is indicated by a dashed line on the simulation. (d) As (b) but the beam size is enlarged to $250 \times 250 \mu\text{m}^2$. The Kossel lines disappear and the remaining reflections show a pronounced splitting, mainly in two almost perpendicular directions. The inset shows an enlarged Laue spot. (e) As (c) but an icosahedral AlPdMn quasicrystal has been used.

approximants.† Furthermore, it is of interest that this 'perfect' sample also shows distinct diffuse scattering.

The stepwise enlargement of the beam size from $70 \times 70 \mu\text{m}^2$ to $250 \times 250 \mu\text{m}^2$ leads to a drastic change in the case of the $\text{Al}_{62}\text{Co}_{15}\text{Cu}_{20}\text{Si}_3$ sample, whereas the pattern of AlCoNi remains almost unchanged. Fig. 2(d) shows a recording taken from $\text{Al}_{62}\text{Co}_{15}\text{Cu}_{20}\text{Si}_3$ using a large beam of size $250 \times 250 \mu\text{m}^2$. The Kossel lines have disappeared and the Laue spots and the diffuse line exhibit a distinct multiple splitting. Consequently, at least near the surface (depths down to some tens of micrometres), the sample is a typical representative of a mosaic crystal. The recording obtained with the largest beam, $250 \times 250 \mu\text{m}^2$, reveals that actually several tens of grains with slightly different orientations are contributing to the diffraction process.

As soon as the exciting beam hits several crystallites which are slightly tilted to each other, the Kossel lines split and the intensity of the single lines decreases until they cannot be distinguished from the background anymore. The vanishing of the Kossel lines is connected to their small excess intensities in general. Laue spots possess much higher intensities and the splitting does not necessarily lead to the disappearance of the spots in the background.

From the deviation of the Laue reflections relative to the ideal positions of the spots, the tilt angles of the mosaic grains were calculated. The maximum tilt angles parallel and perpendicular to the tenfold axis were calculated to be 1.3 and 0.6° , respectively. These values are in good agreement with the results of earlier measurements (Schetelich, 1995). An interesting feature is the distribution of the tilt directions. They are closely related to particular crystallographic directions and not statistically distributed.

Furthermore, it was found that the structure of the spots belonging to the same reflection is not uniform, whereas in directions normal to the tenfold axis the distribution is rather dense, where there is a discrete set of about ten spots parallel to this axis. Decreasing the beam size, a considerably smaller number of splits in both directions is obtained. Their minimal thickness can be roughly estimated by taking the mean excitation depth $z = \mu^{-1}$ (where μ is the absorption coefficient) of the fluorescence radiation, which causes the Kossel interferences ($\text{Co } K\alpha$ and $\text{Cu } K\alpha$, respectively), into account. The excitation depth z was calculated to be about $40 \mu\text{m}$. The minimal lateral dimensions of a single grain are somewhat smaller than $70 \times 70 \mu\text{m}^2$, derived from the initial appearance of the 'light-dark' fine structure of the Kossel lines. Taking results from other Kossel experiments into account (Schetelich, 1995), we deduce that the actual samples consist of a bunch of several quasicrystalline or microtwinned needles.

This particular kind of growth has been described before (Kortan *et al.*, 1989; Wittmann, 1997), but crystallite sizes and tilt angles have not been determined so far. The investigation of the quality of these needles has been carried out by means of the electron-induced Kossel effect at a lateral resolution of approximately $10 \mu\text{m}$ (Weber *et al.*, 1994). The Kossel pattern obtained in this way shows extremely sharp lines with a 'light-dark' contrast due to dynamical diffraction. Dependent on the Bragg angle, even some ($\text{Co } K\alpha$) line doublet splitting was observed as well (angular difference $\sim 0.06^\circ$). The simulation of these patterns revealed lattice parameters as follows: $c = 0.4141$ (5) nm and $a = 0.3776$ (8) nm. These values are in good agreement with the lattice parameters of $\text{Al}_{62}\text{Co}_{15}\text{Cu}_{20}\text{Si}_3$ obtained from the present experiments (Fig. 2c). It can also be concluded that the composition of the single crystallites within the samples does not differ particularly. This is in agreement with results of high-precision density measurements on the same sample. The measured density of $\rho_{\text{exp}} = 4.53$ (3) g cm^{-3} has been simulated using the experimentally determined lattice parameters and the structure model proposed (Kloess *et al.*, 1994). Later, other Kossel experiments proved the occurrence of the effect of an anomalous absorption (Borrmann effect). Therefore, a lateral dimension of the coherent scattering domains of approximately $100 \mu\text{m}$ could be estimated (Schetelich, 1995).

From all these measurements, electron-induced and synchrotron excitation Kossel experiments alike, we found that the samples possess, at least locally, a very high degree of structural perfection. The question, whether the grains are really quasicrystalline or merely microtwinned approximants, cannot be answered in this way, because of the possibility of phase conservation in coherent twinned crystals (Fettweis *et al.*, 1995).

Similar experiments were carried out on $i\text{-AlPdMn}$ and $i\text{-ZnMgY}$. Quasicrystals of this type are without translation symmetry in all three dimensions. The Laue photographs obtained do not show any distinctive diffuse scattering. However, the crystals exhibit a mosaic structure as can be seen from the recordings given in Fig. 2(e). Compared with Fig. 2(d), another type of mosaic structure was found. By decreasing the beam diameter, additional Kossel lines with the fine structure were observed. This is of particular interest in the case of the AlPdMn sample where the electron excitation of the $\text{Pd } K$ -fluorescence radiation failed due to the lack of a source providing an electron beam of a sufficiently high energy (Brenner *et al.*, 1996).

4. Summary

Laue experiments on quasicrystals using a quite unusual experimental set-up were performed. A high spatial resolution was achieved by incorporating a large distance between the film and the sample. Different beam diameters and the combination of Laue diffraction, the Kossel effect and diffuse scattering made it possible to obtain a

† Periodic approximants of the decagonal quasicrystals are an intermediate state between decagonal quasicrystals and ordinary crystals: they have approximately tenfold diffraction patterns, but are in fact periodic crystals with large unit cells (Kalning *et al.*, 1994).

more localized picture from the real structure of the quasicrystalline sample. In the case of a mosaic crystal, the tilt angles and dimensions of the mosaic blocks could be estimated. The mosaic structure of the crystals reveals the dynamical diffraction in these samples as a very localized phenomenon in many cases.

We would like to thank R. Wittmann, S. Kek and A. P. Tsai for providing the samples and useful discussions, W. Morgenroth for his help during the time at station F1, and M. Kalning for discussions regarding the nature of the $\text{Al}_{70}\text{Co}_{15}\text{Ni}_{15}$ sample. The financial support by the Fonds der Chemischen Industrie and the DFG is gratefully acknowledged.

References

- Borrmann, G. (1936). *Ann. Phys.* **5**(27), 669–693.
- anner, S., Schetelich, Ch. & Geist, V. (1996). *Phys. Status Solidi A*, **157**, 23–35.
- Fettweis, M., Launois, P., Reich, R., Wittmann, R. & Denoyer, F. (1995). *Phys. Rev. B*, **51**, 6700–6703.
- Gog, T., Bahr, D. & Materlik, G. (1995). *Phys. Rev. B*, **51**, 6761–6764.
- Kalning, M., Kek, S., Burandt, B. & Steurer, W. (1994). *J. Phys. Condens. Matter*, **6**, 6177–6187.
- Kalning, M., Press, W. & Kek, S. (1995). *Philos. Mag. Lett.* **71**, 341–349.
- Kek, S. & Mayer, J. (1993). *Z. Kristallogr.* **205**, 235–253.
- Kloess, G., Schetelich, Ch., Wittmann, R. & Geist, V. (1994). *Phys. Status Solidi A*, **144**, K5–9.
- Kortan, A. R., Thiel, F. A., Chen, H. S., Tsai, A. P., Inoue, A. & Masumoto, T. (1989). *Phys. Rev. B*, **40**, 9397–9399.
- Schetelich, Ch. (1995). Thesis, University of Leipzig, Germany.
- Schetelich, Ch., Weber, S. & Geist, V. (1994). *Phys. Status Solidi A*, **145**, 51–59.
- Schetelich, Ch., Weber, S., Geist, V., Schlaubitz, M., Ullrich, H.-J., Kek, S. & Krane, H. G. (1995). *Nucl. Instrum. Methods*, **B103**, 236–242.
- Steurer, W. (1990). *Z. Kristallogr.* **190**, 179–234.
- Takahashi, T. & Takahasi, M. (1993). *Jpn. J. Appl. Phys.* **32**, 5159–5162.
- Ullrich, H.-J., Schlaubitz, M., Friedel, F., Spann, T., Bauch, J., Wroblewski, T., Garbe, S., Gaul, G., Knoechel, A., Lechtenberg, F., Rossmannith, E., Kumpat, G. & Ullrich, G. (1994). *Nucl. Instrum. Methods*, **A349**, 269–273.
- Weber, S., Schetelich, Ch. & Geist, V. (1994). *Cryst. Res. Technol.* **29**, 727–735.
- Wittmann, R. (1997). Personal communication.